Ecotoxicology and Environmental Safety 272 (2024) 116015

Contents lists available at ScienceDirect

Ecotoxicology and Environmental Safety

journal homepage: www.elsevier.com/locate/ecoenv

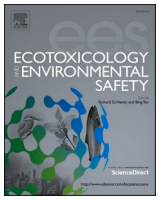

Assessment of co-contaminated soil amended by graphene oxide: Effects on pollutants, microbial communities and soil health

V. Peña-Álvarez [a,b], D. Baragaño [c,*,1], A. Prosenkov [a,b], J.R. Gallego [d], A.I. Peláez [a,b]

[a] Area of Microbiology, Department of Functional Biology and Environmental Biogeochemistry and Raw Materials Group, University of Oviedo, Spain
[b] Institute of Biotechnology of Asturias (IUBA), University of Oviedo, Spain
[c] School of Mines and Energy Engineering, University of Cantabria, Blvr. Ronda Rufino Peón 254, 39300 Torrelavega, Cantabria, Spain
[d] INDUROT and Environmental Biogeochemistry and Raw Materials Group, Campus of Mieres, University of Oviedo, Mieres, Spain

ARTICLE INFO

Edited by: Dr R Pereira

Keywords:
Soil remediation
Graphene oxide
Biostimulation
DNA fingerprinting
Soil pollution

ABSTRACT

Graphene oxide (GOx) is a nanomaterial with demonstrated capacity to remove metals from water. However, its effects on organic pollutants and metal(loid)s present in polluted soils when used for remediation purposes have not been extensively addressed. Likewise, few studies describe the effects of GOx on edaphic properties and soil biology. In this context, here we assessed the potential of GOx for remediating polluted soil focusing also on different unexplored effects of GOx in soil. To achieve this, we treated soil contaminated with concurrent inorganic (As and metals) and organic pollution (TPH and PAHs), using GOx alone and in combination with nutrients (N and P sources). In both cases increased availability of As and Zn was observed after 90 days, whereas Cu and Hg availability was reduced and the availability of Pb and the concentration of organic pollutants were not significantly affected. The application of GOx on the soil induced a significant and rapid change (within 1 week) in microbial populations, leading to a transient reduction in biodiversity, consistent with the alteration of several soil properties. Concurrently, the combination with nutrients exhibited a distinct behaviour, manifesting a more pronounced and persistent shift in microbial populations without a decrease in biodiversity. On the basis of these findings, GOx emerges as a versatile amendment for soil remediation approaches.

1. Introduction

The abandonment of industrial and mining activities has left behind many areas contaminated by metals, metalloids, and hydrocarbons, sometimes even simultaneously. While hydrocarbons are usually degraded into less harmful molecules (Gallego et al., 2022), metals and metalloids are a major threat due to their toxicity, persistence, and bioaccumulation in the food chain (Gong et al., 2020). Traditional physico-chemical soil remediation technologies, such as soil washing or leaching, may negatively affect soil properties and microbiology. Moreover, they are very expensive and not able to completely remove pollutants (Dermont et al., 2008). In contrast, Nature-based Solutions (NBS) such as bioremediation or phytoremediation are low-cost sustainable options for this purpose (Song et al., 2019a).

In this context, soil nanoremediation has recently emerged as a strategy through which to mobilize or immobilize pollutants (Bolan et al., 2014). Nanomaterials are characterized by a large specific surface area and high chemical reactivity (Corsi et al., 2018) and thus they may be more effective in environmental remediation when compared with conventional methods (Alazaiza et al., 2021; Ganie et al., 2021). For instance, iron-based nanoparticles can modify metal and metalloid availability (Fajardo et al., 2019; Mohammadian et al., 2021). In particular, nanoscale zero-valent iron (nZVI) has a high surface area and can immobilize As, Cd, Hg, Pb, and Zn (Fajardo et al., 2020). Also, carbon nanomaterials such as graphene oxide (Baragaño et al., 2020), carbon foams (Janeiro-Tato et al., 2021) or carbon nanotubes (Matos et al., 2017) have been tested for metals immobilization in polluted soils.

Graphene oxide (GOx) is a hydrophilic two-dimensional oxidized form of graphene, resulting from graphite oxidation. Its surface is decorated by oxygen functional groups (Motevalli and Parker, 2019), including epoxide and hydroxyl groups located on the basal plane, and carboxyl and carbonyl groups on the periphery area (Stankovich et al., 2006). GOx is characterized by a high surface area, high density of oxygen functional groups, hydrophobic π-π surface interaction, and

* Corresponding author.
E-mail address: diego.baragano@unican.es (D. Baragaño).
[1] Present address: Instituto de Ciencia y Tecnología del Carbono, INCAR-CSIC, Francisco Pintado Fe, 26, 33011 Oviedo, Spain.

https://doi.org/10.1016/j.ecoenv.2024.116015
Received 31 August 2023; Received in revised form 27 December 2023; Accepted 22 January 2024
Available online 30 January 2024

low-cost production from graphite using chemical oxidation and exfoliation (Futalan et al., 2019). In addition, graphene nanoflakes can be produced from eco-friendly materials (Naik et al., 2020). GOx has proven to be an effective sorbent for metals (Sitko et al., 2013; Wang et al., 2013), and also to remediate aquatic environments (Mishra and Ramaprabhu, 2011; Siddiqui and Chaudhry, 2018). Nonetheless, GOx has received limited attention in the context of soil remediation, despite its potential as an amendment for soil stabilization as demonstrated in a previous work (Baragaño et al., 2020). In fact, the effects of this nanomaterial on soil properties and organic contaminants, or even in plants development, have not been previously addressed.

Potential negative effects of GOx on isolated microorganisms include the inhibition of bacterial growth through the disruption of cell walls and reactive oxygen species production (Akhavan and Ghaderi, 2010; Barrios et al., 2019). Also, some studies have described that GOx can decrease soil enzymatic activity (Chung et al., 2015; Fang et al., 2022) and alter the microbial composition (Forstner et al., 2019), although its effect on bacterial communities in contaminated soils remains ambiguous (Xiong et al., 2018). Conversely, GOx has been described to improve bacterial hydrocarbon biodegradation acting as an electron acceptor (Song et al., 2019b), and it can also enhance microbial growth by providing a large area for attachment (Ming et al., 2019).

On the whole, the interaction of GOx with soil biotic and abiotic components continues still largely unknown. To fill this gap, and to explore GOx uses in soil remediation, here we performed a detailed analysis of a GOx-amended soil contaminated with metal(loid)s and hydrocarbons, also including trials using a combination of GOx and biostimulation with N and P. An exhaustive study of the immobilization of metal (loid)s, degradation of hydrocarbons, edaphic properties and germination index was carried out to assess positive and negative effects on soil health. Also, the Automated Ribosomal Intergenic Spacer Analysis (ARISA) DNA fingerprinting technique was used to evaluate the influence of GOx on soil bacterial communities under the different experimental conditions applied. A multivariate study of all results (bacterial communities and the above referred soil chemical and edaphic parameters) allowed to report novel information about GOx effects in soil and its potential for remediation purposes.

2. Materials and methods

2.1. Graphene oxide characterization

GOx nanoflakes were supplied by Graphenea (San Sebastián, Spain). The nanomaterial was produced using a modified Hummer method (Graphenea's methodology: patent EP15382123 2015).

Different analyses were conducted to characterize GOx: Elemental analysis was performed through a FlashSmart CHNS/O elemental analyser (ThermoFisher) directly on the powder materials. Thermogravimetric analysis (TGA) analysis was performed using a TA Instruments Discovery TGA550 where the dried samples were analysed up to 1000 °C in N_2 atmosphere with a 10 °C/min ramp. XRD was carried out using a Rigaku Miniflex 600 in which dried samples were analysed at 40 Kv and 15 mA with a Cu tube from 7 to 70°. The morphology and microstructure of the nanoparticles were studied by scanning electron microscopy (SEM) directly on the powder using an Environmental Scanning Electron Microscope (ESEM) QuantaTM 250 FEG.

2.2. Soil sampling and initial characterization

Soil was taken from the surroundings of an industrialized area (Trubia, Oviedo) located in Asturias (Northern Spain). A 20-kg composite soil sample was collected from the surface layer (first 25 cm) using a manual auger. In the laboratory, the sample was air-dried, homogenized, and sieved (<2 mm) to remove rocks and debris. The soil was initially analyzed to determine physicochemical properties, total and water-soluble fractions of metal(loid)s, and hydrocarbon concentrations (methodologies described below and results shown in supplementary material, Table S1).

2.3. Microcosm experiments

Microcosm experiments consisted of borosilicate trays of L19xW19xH5 cm containing 250 g of soil. Briefly, the following four treatments were tested (Table 1): control (C); addition of GOx nanoflakes (G); addition of nutrients (N); and combined addition of nutrients and Gox (NG). Each treatment was carried out in triplicate.

As shown in Table 2, GOx nanoflakes were added at a final dose of 2% of the total weight based on previous works (Baragaño et al., 2020); this implied that an additional carbon source was included in G and NG microcosms. In turn, with the nutrients added to microcosms N and NG it was attempted a potential improvement of biodegradation rates of the organic contaminants.

Experiments were conducted at ambient temperature over a period of 90 days, with sample collection at different times (0, 3, 7, 20, 40, 60, and 90 days) for both chemical and microbiological assessment. Moisture was controlled weekly using an MB35 Moisture Analyzer and distilled sterile water was added when needed to keep moisture between 15% and 20%.

2.4. Soil characterization and monitoring

2.4.1. Physico-chemical properties

To study the impact of GOx on soil properties, electrical conductivity (EC), pH, redox potential (Eh), available P, and dissolved organic carbon (DOC) were determined. EC and pH were measured using a METLER TOLEDO SevenCompact™ pH-meter and redox potential (Eh) using an ORP portable meter (HANNA) in a 1:20 soil-water (1 g of soil) suspension after 2 h of shaking. Available P was measured using the Mehlich 3 method (Mehlich, 1984). DOC was determined from 5 g of soil following the method described in Sanchez-Monedero et al., 1996.

2.4.2. Availability of arsenic and metals

Initial metal(loid) concentrations were determined in triplicate representative subsamples of 1 g of soil after acid digestion using a mixture of 6 mL of nitric acid (69% purity) and 2 mL of hydrochloric acid (37% purity), in a microwave reaction system (Milestone ETHOS 1, Italy). In the digestion extract, the concentrations of As, Cd, Cu, Hg, Pb, and Zn were quantified by inductively coupled plasma mass spectrometry (ICP-MS, 7700 Agilent Technologies equipment) using IDA (Isotopic Dilution Analysis) with a spike solution from ISC Science Spain. High-purity standards (Charleston, SC, USA) for calibration and a Certified Reference Material (CRM) (soil, ERM-CC018) were used. Detection limit for all elements is 0.1 μg/l, except for Cu and Zn, which is 0.25 μg/l.

To quantify As and metal availability, subsamples were taken for water extractions from 1 g of soil using a relation of 1:20 w/v and shaken at room temperature for 2 h (Chang et al., 2014; Mench et al., 1994).

Table 1
Experimental microcosm setup according to the soil treatments performed.

Microcosm	Treatment	Description
C	Control (no amendments)	Moisture control and weekly aeration.
G	2% GOx	2% of GOx nanoflakes (dry weight). Moisture control and weekly aeration.
N	Nutrient addition	Ammonium nitrate and sodium dihydrogen phosphate in a C:N:P ratio of 100:10:2. Moisture control and weekly aeration.
NG	Combined nutrients and 2% GOx	2% of GOx nanoflakes (dry weight). Ammonium nitrate and sodium dihydrogen phosphate in a C:N:P ratio of 100:10:2 taking into account the carbon content of GOx. Moisture control and weekly aeration.

Table 2
Physicochemical properties of soil over the 90-day experiment. Different letters in different samples, at the same time-point (columns), indicate significant differences between treatments (n = 3, ANOVA; p < 0.05). Microcosms: control (C), GOx (G), nutrients (N), and combined nutrients and GOx (NG).

Parameter	Units	Treatment	Monitoring time (days)						
			0	3	7	20	40	60	90
EC	μS/cm	C	51.59 ± 1.61	72.86 ± 3.63b	110.32 ± 21.54b	90.04 ± 3.36c	96.47 ± 2.92c	104.50 ± 4.58c	116.20 ± 5.25c
		G	51.59 ± 1.61	117.20 ± 3.31b	132.47 ± 16.21b	137.60 ± 4.52b	159.63 ± 2.18b	161.67 ± 14.00b	181.03 ± 3.75b
		N	51.59 ± 1.61	106.36 ± 5.15b	128.73 ± 3.97b	126.70 ± 3.82b	158.77 ± 5.00b	159.03 ± 3.56b	171.50 ± 2.48b
		NG	51.59 ± 1.61	420.93 ± 32.58a	390.93 ± 13.86a	375.53 ± 6.23a	446.93 ± 12.35a	485.53 ± 6.45a	471.73 ± 22.68a
pH	-	C	6.53 ± 0.04	6.52 ± 0.03a	6.01 ± 0.17a	6.20 ± 0.04a	6.13 ± 0.02a	6.08 ± 0.06ab	6.28 ± 0.04a
		G	6.53 ± 0.04	5.83 ± 0.04c	5.89 ± 0.16a	5.70 ± 0.01c	5.75 ± 0.11b	5.77 ± 0.08b	5.50 ± 0.04c
		N	6.53 ± 0.04	6.30 ± 0.03b	5.97 ± 0.02a	5.90 ± 0.04b	5.76 ± 0.08b	6.21 ± 0.16a	5.82 ± 0.03b
		NG	6.53 ± 0.04	5.89 ± 0.05c	5.72 ± 0.02a	5.69 ± 0.01c	5.48 ± 0.08c	5.38 ± 0.04c	5.33 ± 0.11c
Eh	mV	C	185.97 ± 0.12	185.70 ± 0.96c	186.80 ± 0.26c	184.53 ± 0.55c	196.80 ± 0.70c	190.93 ± 0.44c	191.47 ± 0.87c
		G	185.97 ± 0.12	194.07 ± 0.58a	198.87 ± 0.92a	204.80 ± 0.90a	204.20 ± 0.36b	201.87 ± 1.59b	199.90 ± 0.25b
		N	185.97 ± 0.12	188.77 ± 0.30b	191.97 ± 0.92b	195.00 ± 1.63b	198.63 ± 0.98c	180.47 ± 0.68d	193.27 ± 0.46c
		NG	185.97 ± 0.12	198.23 ± 0.23a	200.13 ± 1.45a	208.87 ± 1.76a	209.93 ± 0.92a	218.47 ± 0.87a	207.50 ± 1.51a
P (available)	mg/kg	C	19.48 ± 1.24	21.14 ± 0.74a	19.03 ± 1.86a	21.56 ± 1.53a	19.71 ± 1.68b	23.83 ± 0.54a	18.96 ± 0.80b
		G	19.48 ± 1.24	20.09 ± 1.37a	23.38 ± 2.94a	22.51 ± 0.90a	20.71 ± 1.53b	22.01 ± 2.56a	20.38 ± 1.42b
		N	19.48 ± 1.24	22.31 ± 1.24a	19.02 ± 2.06a	22.14 ± 2.02a	18.61 ± 1.10b	22.42 ± 2.17a	24.65 ± 1.43ab
		NG	19.48 ± 1.24	28.80 ± 4.02a	28.05 ± 1.85a	27.32 ± 1.62a	26.87 ± 1.59a	29.50 ± 2.89a	27.21 ± 1.43a
DOC	mg/kg	C	7.18 ± 0.61	3.90 ± 0.56a	5.34 ± 0.10a	5.80 ± 0.13a	6.24 ± 0.77a	5.98 ± 0.19b	6.97 ± 0.09a
		G	7.18 ± 0.61	3.77 ± 0.19a	3.57 ± 0.16b	3.84 ± 0.51b	5.12 ± 0.45a	6.44 ± 0.45b	7.28 ± 0.38a
		N	7.18 ± 0.61	4.47 ± 0.05a	4.66 ± 0.18a	6.28 ± 0.36a	5.96 ± 0.53a	6.02 ± 0.30b	11.22 ± 2.06a
		NG	7.18 ± 0.61	5.62 ± 0.61a	5.51 ± 0.52a	5.49 ± 0.71a	6.87 ± 0.62a	10.72 ± 0.41a	7.78 ± 1.02a

Samples were then centrifuged, and the supernatant was passed through a 0.45-μm filter. The concentrations of As, Cd, Cu, Hg, Pb, and Zn were determined by ICP-MS.

As speciation was determined in water extracts, thus As species were separated in a 4.6 mm × 150 mm As Separation Column (Agilent Tech.) fitted to a 1260 Infinity HPLC apparatus coupled to an ICP-MS device using a mobile phase of 2 M PBS (Phosphate Buffered Saline)/0.2 M EDTA (pH = 6.0) at a flow of 1 mL/min.

2.4.3. Organic contaminants

Soil subsamples were analysed to quantify Polycyclic Aromatic Hydrocarbons (PAHs) and total petroleum hydrocarbons (TPH). For PAH determination, 5-g representative subsamples were extracted with dichloromethane:acetone (1:1) in a Soxtherm apparatus (Gerhardt). The extracts were concentrated by rotary evaporation, and the 16 priority PAHs were measured after injection into a 7890 A GC System coupled to a 5975 C Inert XL MSD with a Triple-Axis Detector (Agilent Technologies) and following a modification of EPA method 8272. A capillary column DB-5 ms (5% phenyl and 95% dimethylpolysiloxane) 30 m × 0.25 mm i.d. × 0.25 μm film (Agilent Technologies) was used, with He as carrier gas at a flow rate of 1 mL/min. The initial oven temperature was 80 °C (held for 2 min), which was ramped up at 15 °C/min–300 °C (held for 10 min). The GC injector was operated in splitless mode for 2 min at 260 °C. The mass spectrometer was operated in selected ion monitoring mode (SIM), and the quantification *m/z* relations were 128, 152, 153, 154, 165, 166, 178, 202, 228, 252, 276, and 278. The extracts were also measured in the same GC–MS apparatus with the same column to quantify semivolatile (C10-C40) TPH, following EPA Method 8270 C. In this case, the initial oven temperature was 40 °C (held for 5 min), which was ramped up at 5 °C/min–300 °C (held for 20 min). The chromatograms were acquired in full-scan mode (mass range acquisition from 45 to 500 *m/z*). In both cases, the MS was operated in electron ionization mode (EI) at 70 eV and calibrated daily by auto-tuning with perfluorotributylamine (PFTBA) and calibration mixtures (AccuStandard and Ehrenstorfer respectively) were used.

2.4.4. DNA fingerprinting of bacterial communities

DNA was extracted in triplicate from the initial soil and the replicates of each treatment using the PowerSoil DNA Isolation Kit (Qiagen) from 0.25 g of soil following the manufacturer's instructions. A total of 75 samples were processed. Automated Ribosomal Intergenic Spacer Analysis (ARISA) (Fisher and Triplett, 1999) was used to assess changes in bacterial community structure during the microcosm experiments. The 16 S to 23 S rRNA intergenic spacer region was amplified using specific ARISA Primers ITSReub (5'-GCCAAGGCATCCACC-3') and ITSF (5'-GTCGTAACAAGGTAGCCGTA-3') labelled with a fluorescent dye (HEX or 6FAM) (Cardinale et al., 2004). For the PCR reaction, Speedy Supreme NZYTaq polymerase (NZYTech) was used according to the manufacturer's instructions, using 5 ng of DNA template, annealing temperature of 55C, and final extension prolonged to 10 min. Fragment study was performed on an ABI PRISM 3130xl Genetic Analyzer (Thermo Fisher) using GS500 (ROX) size standard. Electropherogram data were visualized and analyzed with Peak Scanner™ Software v1.0. Background noise thresholds were set to 50 fluorescence units and any peak below this threshold was discarded.

OTU (Operational Taxonomic Units) binning was performed with R *interactivebinner.r* script (Ramette et al., 2009), using fragments between 200 and 1000 base pairs (bp) and a minimum Relative Fluorescent Intensity (RFI) cutoff value of 0.09%. Differences between bacterial communities were analyzed by calculating a Bray-Curtis dissimilarity matrix using R package *vegan* (Oksanen et al., 2012). Based on this matrix, non-metric multidimensional scaling (NMDS) ordination and analysis of similarities ANOSIM (Clarke, 1993) were used to evaluate differences between groups. A Shepard diagram was generated to explore the goodness of fit of data in the NMDS ordination chart (Shepard, 1962). To estimate the effect on abiotic soil proprieties, a Mantel test (Mantel, 1967) based on Spearman correlation was carried out with 9999 permutations. Also, indicator species analysis (De Cáceres et al., 2010) was performed to highlight OTUs significantly associated with one or more treatments. Using the *hilldiv* R package (Alberdi and Gilbert, 2019), Hill numbers (q=0, q=1, and q=2) were calculated to explore changes in alpha-diversity of microbial communities (Hill, 1973; Roswell et al., 2021). E2.0 community evenness was calculated as a ratio between Hill numbers q= 2 and q= 0.

2.4.5. Germination index

To assess the impact of GOx on plant germination, the germination index of the *Lepidium sativum* seeds was determined using a modified version of the Zucconi test (Zucconi et al., 1981; Zucconi et al., 1985). Briefly, six *Lepidium sativum* seeds were moistened either with 6 mL of distilled water (for the control), soil extract or 2% w/v GOx suspension and were then placed onto filter paper inside Petri dishes. Extracts were obtained by adding 50 mL of distilled water at 60 °C to 5 g of soil for 30 min, followed by filtering with a Whatman paper (541 grade). After an incubation period of 72 h in darkness at 25 °C, the germination index (GI) was determined:

$$GI(\%) = \frac{GxL_s}{L_c} \quad (1)$$

Where G is the percentage of germinated seeds (root length higher than 5 mm), L_s is the mean root length in the soil extract, and L_c is the mean root length in the control. Tests were performed in triplicate.

2.5. Statistical analysis

The data obtained were statistically treated using SPSS version 25.0 for Windows. Analysis of variance (ANOVA) and test of homogeneity of variance were performed. In the case of homogeneity, a post hoc least significant difference (LSD) test was carried out (Williams and Abdi, 2010). If there was no homogeneity, Dunnett's T3 test was performed (Dunnette, 1963).

Principal Component analysis (PCA) and factor analysis (FA) were carried out to identify possible interrelations between parameters and groups. The PCA was done in R software (version 4.1.1) with the *FactoMineR* package (Lê et al., 2008) while FA was performed using the *fa* function included in the *Psych* package (Revelle, 2015). To evaluate the adequacy of the data set, a Kaiser-Meyer-Olkin (KMO) test was carried out (Kaiser and Rice, 1974). Finally, to evaluate the concordance between NMDS and PCA ordinations, Procrustes analysis (Gower, 1975) was performed with 9999 permutations.

3. Results and discussion

3.1. Graphene oxide characterization

According to CHNS/O determination, the graphene oxide powder revealed a composition of 52.49% of C, 43.41% of O, 1.63% of H, 0.02% of N and 2.47% of S.

The XRD pattern of graphene oxide powder is shown in Fig. S1 in the supplementary material. The main diffraction peak of graphene oxide appeared at the range 9.0–11.20°, whereas the main one of graphite (26°) was absent thereby assuring that the transformation of graphite into graphene oxide was complete. The TGA plot (Fig. S1) also confirmed the purity of the product as the main weight loss was found around 200 °C corresponding to the decarboxylation of graphene oxide (Baragaño et al., 2020 and references therein). Finally, SEM revealed the distinctive flake shape of GOx (Fig. S2).

3.2. Initial soil characterization

The properties of the polluted soil are shown in Table S1. Soil characteristics revealed a high content of organic matter, which suggests a healthy structural status. According to the pH and electrical conductivity (EC) values, the soil was slightly acidic and non-saline (Hazelton and Murphy, 2016). Regarding As and metal content, only As and Pb exceeded the Risk-Based Soil Screening Levels (RBSSLs) established in the region of Asturias for all soil uses, whereas Hg levels exceeded the limits for urban and natural soil land use (those suitable for agricultural, forestry, and livestock-raising activities; BOPA, 2014). According to the water extraction, As was the most mobile pollutant in the soil, although the percentage of leachability was not high.

With regard to organic pollutants, a notable presence of hydrocarbons of between 16 to 35 carbon atoms was found (Table S1). Most of these hydrocarbons were the 16 priority PAHs Among the 16 priority PAHs (ATSDR, 2005). Of note, Benzo(b)fluoranthene, Benzo(a)pyrene, Dibenzo(a,h)anthracene, and Indene(1, 2, 3-cd)pyrene were clearly above the RBSSLs (RD 9/2005, 2005). The chromatogram shown in Fig. S3 shows the absence of readily degradable compounds such as linear alkanes, and the predominance of recalcitrant heavy PAHs.

3.3. Evolution of soil parameters

Electrical conductivity (EC) generally showed an increasing trend in all treatments over the 90-day experiment although the initial increase in N, G, and NG treatments was abrupt and, in some cases, slight fluctuations were observed. This phenomenon may be attributed to the introduction of electrically active compounds such as nutrients and GOx. Notably, there was no substantial difference in EC from day 3 to the end of the experiment in N, G and NG treatments. In contrast, the control group exhibited a gradual increase in EC throughout the experiment, although it never reached the higher levels observed in the N, G, and NG treatments (Table 2). Soil pH showed an initial decrease in most treatments that was maintained until the end of the experiment with soft fluctuations, this was mainly observed in those treatments involving GOx (G and NG, final pH below 5.5 in both cases) as a result of the acidic nature of GOx nanoflakes (Baragaño et al., 2020) (Table 2). Redox potential (Eh) at the beginning of the experiments was oxidative and this parameter increased gradually over time, showing some variations in all experiments (Table 2). However, the slight increase observed in the G and NG treatments was significantly higher than in C, thereby indicating that GOx modified the oxidation conditions of the soil likely due to its behaviour as redox mediator (Song et al., 2019b and references therein). Although the variations in Eh and pH caused by GOx were not considerable, the combination of both could favour the mobilization of some pollutants (Frohne et al., 2011). Available P content was moderately higher after 90 days in the N and NG treatments due to the addition of salts whereas no relevant differences were observed between the C and GOx treatments (G) (Table 2). Therefore, in contrast to previous studies (Baragaño et al., 2020), GOx amendment did not cause an increase in P availability. This result is important given that phosphate is chemically analogous to arsenate, and thus changes in P availability could alter As mobility (Beesley et al., 2014). Finally, DOC varied depending on the treatment and sampling time but did not show a clear pattern.

3.4. Availability of arsenic and metals

The availability of As, Cd, Cu, Hg, Pb, and Zn in was monitored throughout the experiment. No detectable levels of Cd were observed in the water extractions. The availability of As in the microcosm experiments increased with GOx addition; the NG treatment showed the highest rise, whereas the C and N treatments revealed a slight decrease (Fig. 1). These effects were observed in the three first days of the experiment and persisted until day 90. As was present mainly in its most oxidized form, As(V), which exceeded 95% in all measurements, without any significant changes in any treatment; this is consistent with the oxidative condition of the soil (Camm et al., 2004; Siddiqui and Chaudhry, 2018).

On the whole, there was an increase in As availability when GOx was added. GOx has a zero-point charge (ZPC) of around pH 2.0, and at a higher pH it is deprotonated, revealing a negatively charged surface (Mondal and Chakraborty, 2020), as occurred in this study given that the soil pH was around 5.5. Since both ions in the solution and the surface of the deprotonated graphene oxide are negatively charged, they repel each other due to electrostatic forces and promote As mobilization (Siddiqui and Chaudhry, 2018; Baragaño et al., 2020). In turn, arsenate (As(V)) and P are chemically analogous, so they can compete in soil

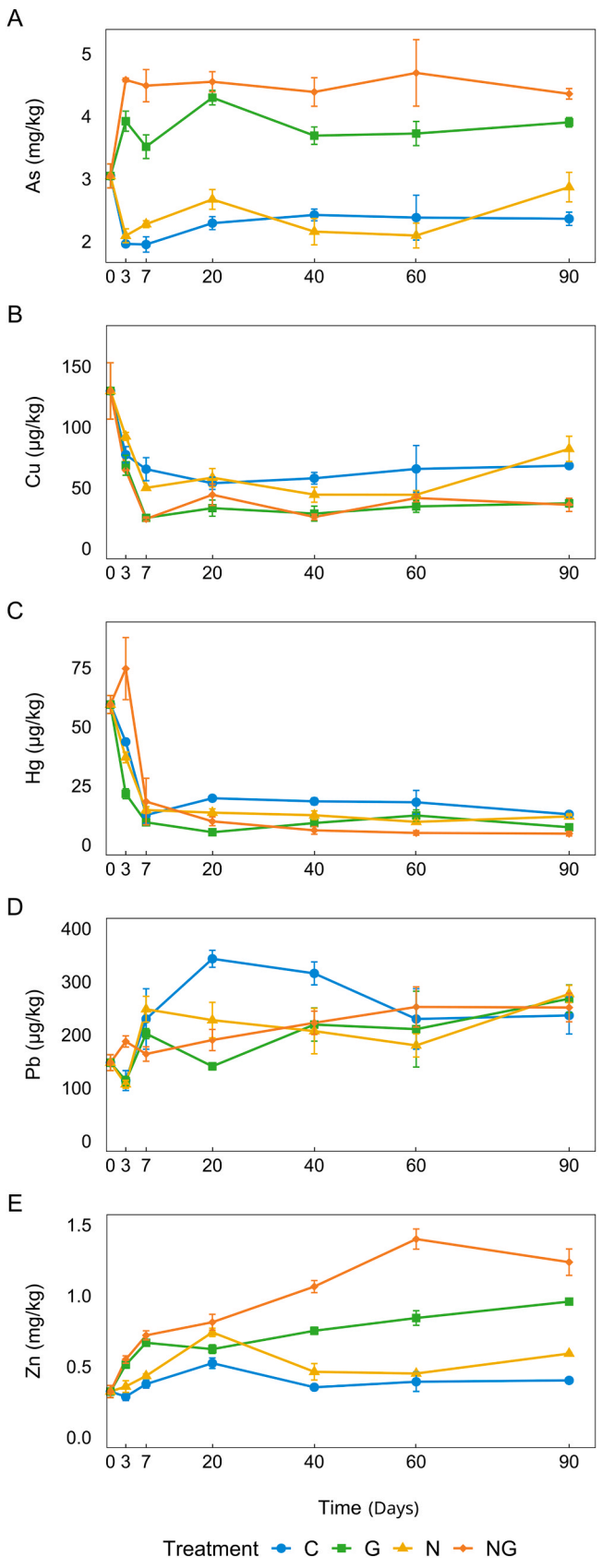

Fig. 1. Available concentrations of As, Zn, Cu, Hg, and Pb over time. C: control, G: GOx, N: nutrients, NG: combined nutrients and GOx. The numerical data and significant differences are detailed in Table S2.

systems for binding (Beesley et al., 2014; Strawn, 2018) and may facilitate As removal from soil particles (Baragaño et al., 2020). In our study, we observed a correlation between As and P (0.7, $P < 0.01$) in the NG treatment, which is not observed in the G treatment. This correlation could explain the higher rate of mobility in the case of NG. On the other hand, the available As in the N microcosm did not differ from the control, suggesting that a higher available P concentration alone may not be sufficient to mobilize As in this soil. Notably, As (V) was found as the only As species present in the soil extracts.

Concerning Zn availability, this metal gradually increased throughout the experiment in GOx-treated soils, especially in the NG microcosm, whereas only a relatively small increase was observed in the C and N treatments, without significant differences after 90 days in comparison with the initial concentration. Some studies have described GOx as an effective adsorbent to Zn ions (Ain et al., 2019; Futalan et al., 2019; Najafi, 2015). However, this capacity is closely related to optimum pH values of around 7, while at pH 5 only 20% of adsorption capacity is observed (Ain et al., 2019; Wang et al., 2013). This reduced adsorption at acidic pH is due to the competition between protons and Zn (II) ions in water solutions (Lei et al., 2014), and a similar effect has been observed in soil amended with organic products (Houben et al., 2013); i.e., a decrease in soil pH caused Zn mobilization. In our study, this was corroborated by a negative correlation (−0.8, $P < 0.01$) between Zn availability and pH when GOx was added to the soil.

Regarding Cu, Hg and Pb, only slight differences were observed between treatments. Cu mobility decreased in all treatments, most notably in those involving GOx (G and NG) that showed a slightly significant lower availability after 90 days. In this sense, the optimum pH range for Cu adsorption to GOx in water is between 3 and 7 (Wu et al., 2013), and the pH of the tested soil fell in this range, thereby favouring Cu immobilization. We hypothesize that the oxygen atoms of the functional groups on the negative surface of GOx donate their only pair of electrons to the Cu ions, thus achieving Cu immobilization (Baragaño et al., 2020). A similar behaviour was found for Hg, which was immobilized after GOx (G and NG) application, thus similar immobilization mechanisms to those of Cu may be involved. In contrast, Pb availability fluctuated in all the soil treatments, although some trends were found. In the short-term, Pb availability was lower in the G than in the C treatment. This observation could be explained by the immobilization mechanism reported by Baragaño et al. (2020), although in the long-term Pb was remobilized.

3.5. Organic pollution

Total petroleum hydrocarbons (TPH) barely decreased in any of the treatments, and only a slight (but statistically significant) reduction in the N treatment was observed, possibly due to biodegradation. This decrease was more accentuated for hydrocarbons with more than 30 carbon atoms and some PAHs (Table S3), but it cannot be linked to the addition of GOx.

In aqueous environments, natural organic matter (NOM) reduces the ability of graphene-based nanocomposites to adsorb organic compounds (Apul et al., 2013; Lu et al., 2018). In the context of organic and inorganic co-pollution, GOx appears to have a higher affinity for metals (Wang and Chen, 2015). In addition to the referred precedents, in our case, the hydrocarbons found in the soil were not easily biodegradable, as described above.

3.6. Effects on soil microbiology

Molecular fingerprinting techniques allowed to carry out a straightforward study of the microbial community structures in the presence and absence of GOx. ARISA provides a community-specific binding pattern (Dubey et al., 2020) and a reliable examination of changes (Castaño et al., 2021; Gallego et al., 2022; Mahamoud Ahmed et al., 2018; Ranjard et al., 2006) that is reflected in the segregation of microbial communities in each treatment over time (Fig. 2). Bacterial

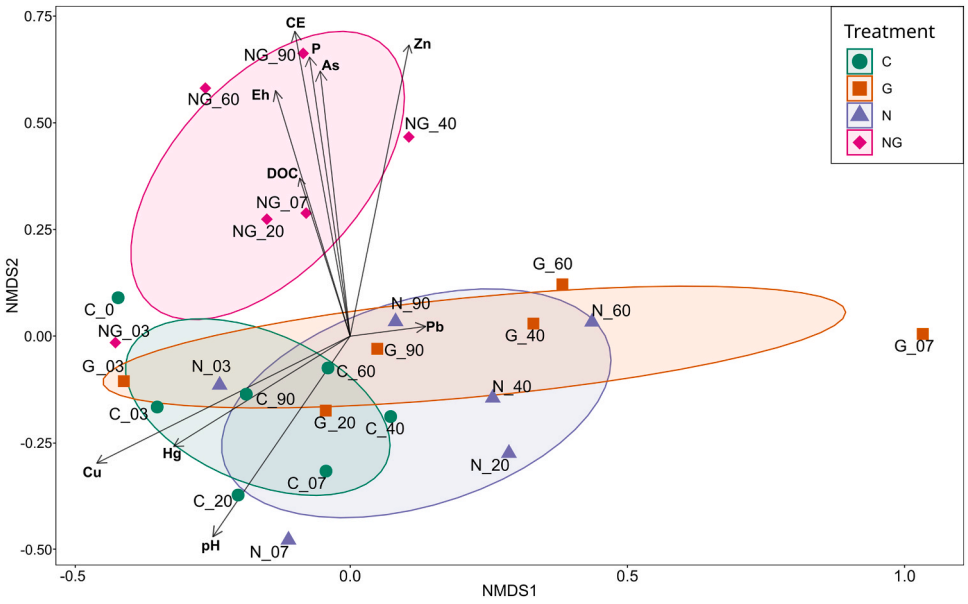

Fig. 2. Non-metrical Multidimensional Scaling (NMDS) ordination plot of Bray-Curtis community dissimilarity matrix obtained from bacterial ARISA profile (Shepard plot non-metric fit = 0.971, stress value = 0.17). NMDS illustrate differences in the structure of bacterial communities in each treatment over time. Axes represent arbitrary distances. Environmental vectors (arrows) were fitted onto NMDS ordination. Length and direction show the strength of the linear correlation of environmental variables and microbial data (longer segments show a higher correlation with the data). Ellipsis areas represent 60% of confidence. Microcosms: control (C), GOx (G), nutrients (N), and combined nutrients and GOx (NG).

profiles on day 0 and day 3 were very similar in the NMDS ordination chart, indicating the same bacterial community structures. However, they started to move away from the initial soil pattern (C0) after 7 days. These changes were more pronounced in the case of microcosms involving GOx, thereby suggesting strong disturbances not maintained over time in microcosm G as communities converged to those of C in the following sampling times. These observations are consistent with previous studies in which GOx addition modified microbial communities only transiently (Chung et al., 2015; Du et al., 2015; Ren et al., 2015; Xiong et al., 2018).

On the other hand, as shown in Fig. 2, for the NG treatment, this alteration was maintained over 90 days, suggesting that changes in microbial communities likely reflected adaptation to new environmental conditions (not only GOx presence but higher availability of nutrients) (Du et al., 2015). Comparison of the distribution of microbial communities in the NG microcosms with key environmental parameters using the NMDS plot (Fig. 2) revealed a positive correlation with EC, available Zn, available P, available As, and Eh, as shown by the environmental vectors represented in the figure. In addition, a Mantel test was carried out to evaluate the correlation between bacterial communities and each environmental factor, which was significant for EC ($R = 0.5479$, $p = 0.0001$), Eh ($R = 0.4192$, $p = 0.0002$) and available P ($R = 0.408$, $p = 0.0002$). In contrast, the mobilization or immobilization of metal(loid)s in the soil had a much lower correlation with the structures of communities, possibly due to the high tolerance of native bacteria to the pollutants (complete Mantel test scores are shown in Table S4). Thus, parameters such as EC, Eh and P could have had the highest influence on the divergence of bacterial communities in the NG treatments.

From a different perspective, according to the ANOSIM test, the time of sampling did not affect bacterial communities ($p > 0.001$), and the corresponding R-ANOSIM value was low ($R = 0.1633$), thereby indicating a low degree and speed of change. In contrast, the amendments added to the soil had a much stronger effect on bacterial community structure ($R = 0.4398$; $p = 0.0001$).

In turn, Hill numbers (Alpha-diversity) were calculated to determine whether any treatment had an impact on the richness and evenness of bacterial communities (Fig. 3). Hill numbers modulate the weight of OTU frequencies by changing the "order", i.e., the higher the q value, the greater the importance of OTU frequency (Alberdi and Gilbert, 2019). Therefore, Hill number $q = 0$ is insensitive to OTU frequency and thus is used as a richness metric, $q = 1$ is equivalent to an exponential of the Shannon index, and $q = 2$ is equivalent to the inverse of the Simpson index. Community evenness (E2.0) was therefore calculated as a ratio of $q = 2$ to $q = 0$. In this regard, from the richness-evenness scatterplot, as in the case of NMDS ordination, samples from the NG treatment were grouped away from the rest (Fig. 3A). They showed higher community richness with low evenness, suggesting that the communities were dominated by a small number of organisms. Conversely, on day 7 after GOx addition, the G microcosm revealed low community richness with high evenness, probably due to a reduction of OTU counts. Hill numbers $q = 1$ and $q = 2$ (Figs. 3B and 3C) decreased in all cases compared with the initial soil. Moreover, treatments displayed lower values of alpha-diversity in comparison to the control. In all treatments, alterations in soil conditions such as pH (in G and NG treatments), EC (in G, N, and NG treatments), Eh (in G and NG treatments), or nutrient source (in N and NG treatments) could result in a specialization of soil bacterial communities. This led to the promotion of the growth of those populations that are better adapted to the new conditions, subsequently reducing diversity. However, it is worth noting that this decline was more pronounced in the initial states of G microcosm, indicating a negative, although transient, impact on diversity seven days after the treatment.

Indicator species analysis showed that of the 57 OTUs obtained from all the treatments, 18 were significantly associated ($p < 0.05$) with one or several treatments (Fig. 4). The greatest change in the relative abundances of the different OTUs appeared on day 7, especially in the G treatment, where many of the OTUs identified at the initial times disappeared, an effect also appreciated in the decrease of richness of sample G_07 (Fig. 3A) as previously explained. In addition, while treatments C, G, and N exhibited some shared OTUs, the NG treatment displayed OTUs (33, 34, 41, 43, 45 and 46) exclusively associated with it. This could be linked, as previously suggested by the NMDS analysis (see above) and in coherence with the Mantel test outcome (see below), to the selection of bacterial strains that are better adapted to the alterations observed in NG for some physicochemical properties (higher availability of As, Zn, and

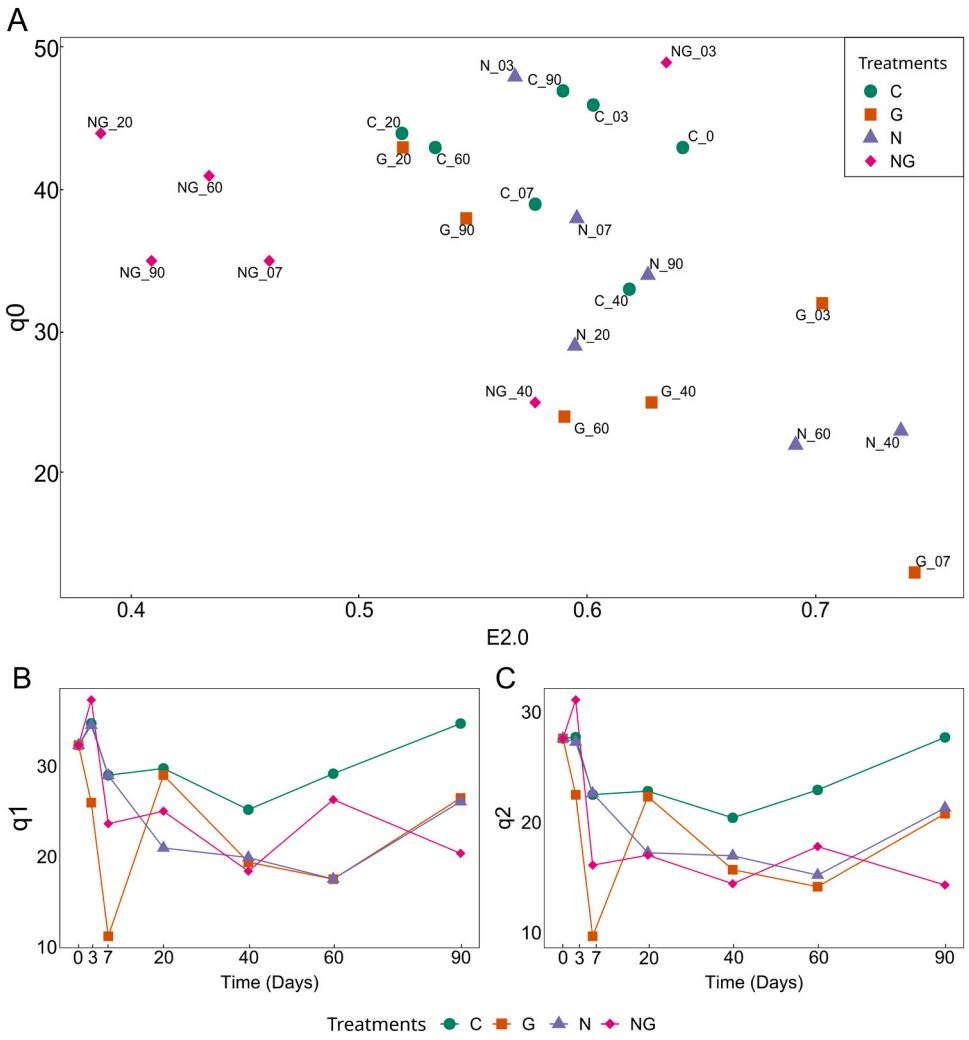

Fig. 3. Alpha-diversity indices of microbial communities in microcosms from samples at different times calculated using ARISA data. A, richness-evenness scatterplot; B, Hill diversity q = 1; C, Hill diversity q = 2. Microcosms: control (C), GOx (G), nutrients (N), and combined nutrients and GOx (NG).

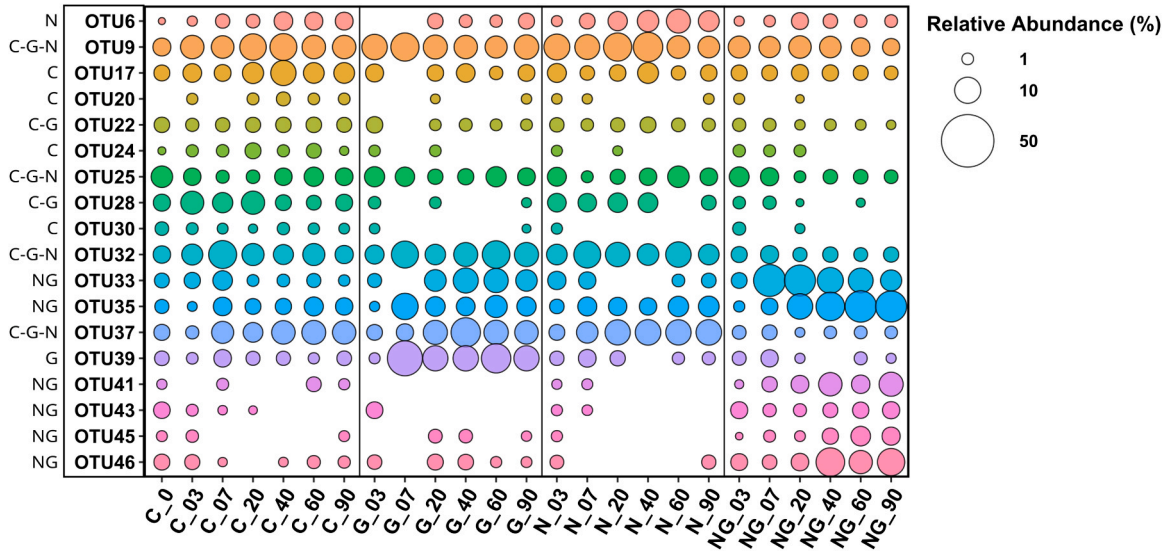

Fig. 4. Relative abundance of OTUs significantly associated with a treatment or group of treatments and their presence in soil bacterial community over time. Left column shows the treatment(s) with which each OTU is associated. Microcosms: control (C), GOx (G), nutrients (N), and combined nutrients and GOx (NG).

P).

Taken together, our findings allow us to conclude that GOx had a transitory negative short-term effect on soil biodiversity. It has been reported that the large number of sharp edges of GOx nanoflakes may damage the bacterial membrane (Akhavan and Ghaderi, 2010; Efremova et al., 2015). However, over time, the interaction between GOx and soil microorganisms could modify the surface of the nanomaterial by increasing its thickness and producing other organic molecules, nitrogen-containing groups, and fewer negative charges, resulting in less harmful effects (Du et al., 2015). Such an ageing process occurs over time when GOx is added to the soil, although we propose that the simultaneous addition of GOx and nutrients could speed it up. This consideration may explain why no negative effects on bacterial communities were identified in the NG treatment.

3.7. Multivariate study

A dataset of 25 samples and 10 variables were obtained during the microcosm experiments and as explained above, it was not easy to identify the parameters most affected by the amendments. Therefore, we applied a PCA and FA, powerful and versatile statistical methods (Bro and Smilde, 2014), to further discuss the results.

The PCA (Fig. 5) reported three major components, accounting for 82.8% of the total variance. PC1 represented 50.2% of the variance, with the highest loads for Zn availability (0.932), EC (0.882), Eh (0.814), and As availability (0.800). The highest loads in PC2 (18.3% of variance) and PC3 (14.3%) were Hg availability (0.790) and DOC (0.825), respectively.

In the PCA (Fig. 5), the N and C treatments were clustered and showed considerable overlap, whereas a lower overlap was observed in the case of the G treatment. However, the NG treatment appeared in a significant and completely different cluster. Differences were therefore consequences of variations in chemical parameters, although changes in, for instance, the availability of Cu and Hg, had a weak effect on the PCA distribution. Accordingly, we can conclude that relevant changes, and mainly those observed in the NG treatment, correspond to the increase in As and Zn availability in correlation with physico-chemical properties of the soil, such as EC, Eh, and available P.

These results were also corroborated by the FA (Table S5). As with the PCA, the FA suggested that EC, P, As, Eh, and Zn had a higher influence on the variations; furthermore, factor 1 (38.5% of variance) grouped the environmental factors that generally increased in the NG treatment (As, CE, Eh, P and Zn), whereas variables that decreased along the experiment were explained by factor 2.

Comparison of the physico-chemical multivariate analysis of the soil with DNA microbial fingerprinting analysis showed a strong similarity between changes in physic-chemical properties of the soil and changes in microbial communities. This resemblance was corroborated by symmetric Procrustes rotation analysis ($R = 0.68$, $p = 0.0004$), revealing a good grade of concordance between the PCA and NMDS ordinations. Furthermore, some of the parameters that most affected the PCA distribution were also the variables that appeared to have a greater influence on changes in bacterial community structure (EC and pH), as determined by the Mantel test. Overall, changes in both microbiological and physic-chemical properties were tightly related and dependent.

3.8. Germination index

The effects of GOx on the germination of *Lepidium sativum* seeds (garden crees) are shown in Fig. 6. Germination index (GI) values below 50% reflect high phytotoxicity, 50% to 80% moderate, and above 80% no phytotoxicity (Zucconi et al., 1985). Initial values revealed high

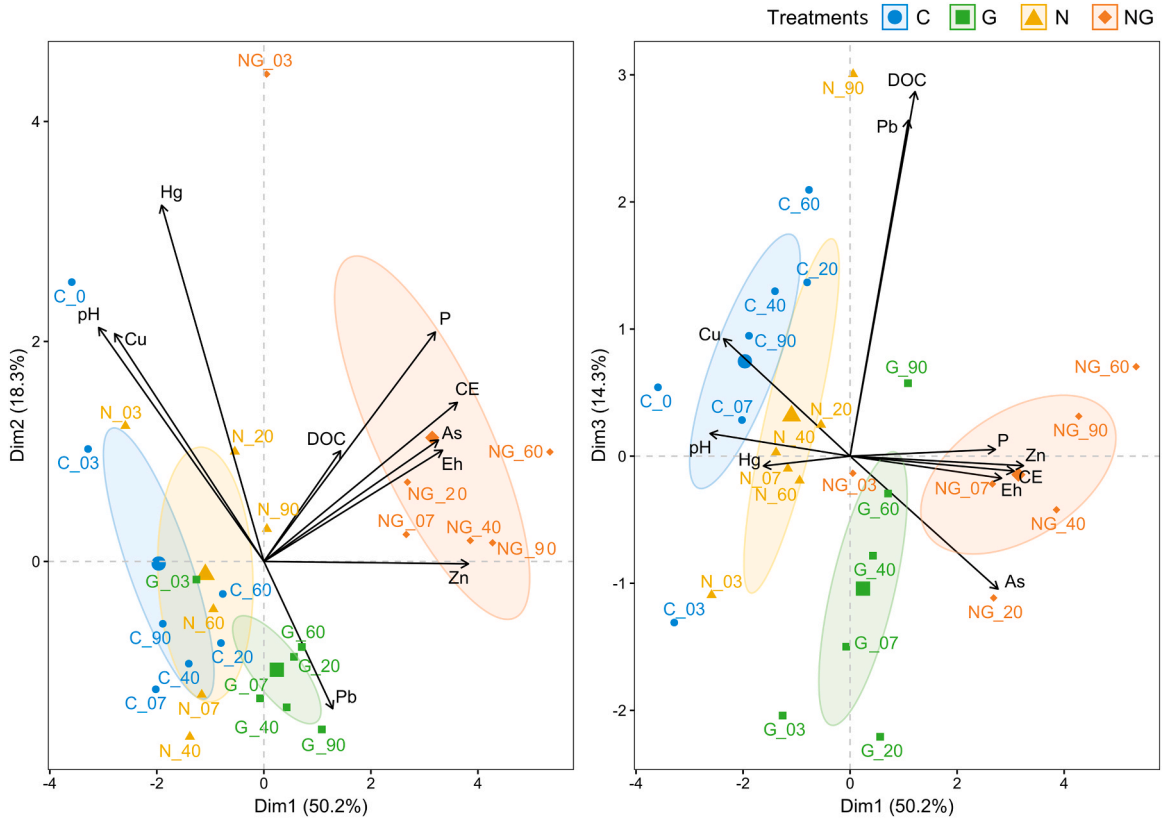

Fig. 5. Principal Component Analysis (PCA) constructed from soil parameters ($P < 0.05$); plots show the three first principal components (the first one is presented in both graphs in the x-axis as it represents more than 50% of the total variance). Arrows show the direction and loadings of variables (longer segments show a higher loading of variables in the dimension). Samples are grouped by confidence ellipses. Microcosms: control (C), GOx (G), nutrients (N), and combined nutrients and GOx (NG).

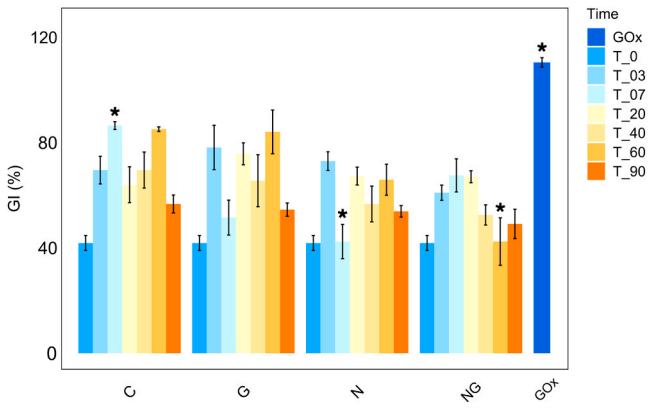

Fig. 6. Evolution of the germination index (%) of *Lepidium sativum* seed in soils treated with the different amendments and a GOx 2% suspension in water (labelled GOx). Asterisks (*) indicate significative differences among treatments sampled at the same time-point. Microcosms: control (C), GOx (G), nutrients (N), and combined nutrients and GOx (NG).

toxicity of the soil (GI = 42%), but over time the GI fluctuated between 50% and 80%, which suggests moderate soil toxicity and therefore an improvement might be attributable to the treatments; however, the values of GI and their variability in the control are comparable with the rest of the treatments and therefore no specific beneficial effect can be deduced from any of them.

Interestingly, a 2%-GOx suspension in water (without soil) showed GI values above 100%. GOx have been described as a water carrier in soil (He et al., 2018) which, together with its ability to penetrate seeds, would facilitate the entry of water and improve germination rates (Zhang et al., 2015). However, this effect is uncertain in the experimental conditions assayed, as no clear improvement of GI index was observed.

Hu et al. (2014) described how GOx amplifies As(V) toxicity in wheat but does not affect germination, but rather weight, root number, and root and shoot length. In our case, the interaction between GOx and phytotoxicity in the soil is difficult to interpret as many variables, discussed above, were modified throughout the experiment, including the pH, EC, and As and Zn availability. In any case, the GI may not be sufficient to comprehensively evaluate the actual effects of GOx on plant growth. Thus, the evaluation of biochemical and physical parameters associated with plant stress, as chlorophyll content, ethylene production, electrical capacitance in root–soil systems or membrane stability index (Füzy et al., 2019) will be necessary to delve deeper into the real effect of GOx.

4. Conclusions

Application of GOx to polluted soil altered the availability of metal (oid)s, effectively mobilizing As and Zn and immobilizing secondarily Cu and Hg, while having minimal effects on recalcitrant hydrocarbons and Pb. Furthermore, GOx, alone or combined with nutrients, promoted significant changes in soil pH, redox potential (Eh), and electrical conductivity (EC), parameters linked to the mobility of the metal(loid)s. These changes are correlated with alterations in soil bacterial communities, as demonstrated using multivariate statistics.

Soil amendment with GOx induced noticeable changes in bacterial communities, particularly 7 days after application a reduced bacterial diversity was observed although in the evolution up to 90 days this effect was attenuated. A different behaviour of the microbial populations was observed in the combination of nutrients and GOx, as the biodiversity was hardly affected but the structure of the bacterial communities changed markedly. Furthermore, GOx did not harm the germination index, although its real effect on plant development requires additional studies.

On the basis of our findings, GOx is a potentially multipurpose material for soil remediation, for instance to stabilize metal-contaminated soils or to enhance As phytoextraction, whereas the effects on organic contaminants should be deeply addressed. Finally, although GOx clearly alters some soil properties, this does not imply a permanent loss of microbial biodiversity (only transient) and may not be a problem for plant growth.

CRediT authorship contribution statement

The corresponding author **D. Baragaño** together with **J.R. Gallego** contributed to the study conception and design. Material preparation, data collection and analysis were performed by **V. Peña-Álvarez**, **A. Prosenkov**, and **D. Baragaño**. The first draft of the manuscript was written by **V. Peña-Álvarez** and all authors commented on previous versions of the manuscript. All authors read and approved the final manuscript.

Declaration of Competing Interest

The authors declare that they have no known competing financial interests or personal relationships that could have appeared to influence the work reported in this paper.

Data availability

Data will be made available on request.

Acknowledgments

This work was funded by the project NANOCAREM (AEI/Spain, FEDER/EU, MCI-20-PID2019–106939GB-I00). We would like to thank the Environmental Assay Unit and Sequencing Unit of the Scientific and Technical Services of the University of Oviedo for technical support. V. Peña-Álvarez acknowledges the Ministerio de Ciencia e Innovacion (MICINN) of Spain for the award of a FPI Grant (PRE2020–093585). Diego Baragaño wants to acknowledge MCIU/AEI/CSIC for his JdC contract under the grant JDC2022-050209-I funded by MCIU/AEI/10.13039/501100011033 and by European Union NextGenerationEU/PRTR.

Appendix A. Supporting information

Supplementary data associated with this article can be found in the online version at doi:10.1016/j.ecoenv.2024.116015.

References

Ain, Q.U., Farooq, M.U., Jalees, M.I., 2019. Application of magnetic graphene oxide for water purification: heavy metals removal and disinfection. J. Water Process Eng. 33, 101044.

Akhavan, O., Ghaderi, E., 2010. Toxicity of graphene and graphene oxide nanowalls against bacteria. ACS Nano 4 (10), 5731–5736.

Alazaiza, M.Y., Albahnasawi, A., Ali, G.A., Bashir, M.J., Copty, N.K., Amr, S.S.A., Al Maskari, T., 2021. Recent advances of nanoremediation technologies for soil and groundwater remediation: a review. Water 13 (16), 2186.

Alberdi, A., Gilbert, M.T.P., 2019. A guide to the application of Hill numbers to DNA-based diversity analyses. Mol. Ecol. Resour. 19 (4), 804–817.

Apul, O.G., Wang, Q., Zhou, Y., Karanfil, T., 2013. Adsorption of aromatic organic contaminants by graphene nanosheets: comparison with carbon nanotubes and activated carbon. Water Res. 47 (4), 1648–1654.

ATSDR. (2005). Agency for Toxic Substances and Disease Registry. Toxicological Profile for Polycyclic Aromatic Hydrocarbons (PAHs), ATSDR's Toxicological Profiles, CRC Press, Boca Raton, FL.

Baragaño, D., Forján, R., Welte, L., Gallego, J.R., 2020. Nanoremediation of As and metals polluted soils by means of graphene oxide nanoparticles. Sci. Rep. 10 (1), 1–10.

Barrios, A.C., Wang, Y., Gilbertson, L.M., Perreault, F., 2019. Structure–property–toxicity relationships of graphene oxide: role of surface chemistry on the mechanisms of interaction with bacteria. Environ. Sci. Technol. 53 (24), 14679–14687.

Beesley, L., Inneh, O.S., Norton, G.J., Moreno-Jimenez, E., Pardo, T., Clemente, R., Dawson, J.J., 2014. Assessing the influence of compost and biochar amendments on the mobility and toxicity of metals and arsenic in a naturally contaminated mine soil. Environ. Pollut. 186, 195–202.

Bolan, N., Kunhikrishnan, A., Thangarajan, R., Kumpiene, J., Park, J., Makino, T., Scheckel, K., 2014. Remediation of heavy metal (loid) s contaminated soils–to mobilize or to immobilize. J. Hazard. Mater. 266, 141–166.

BOPA (2014) Boletín Oficial del Principado de Asturias. Generic reference levels for heavy metals in soils from Principality of Asturias, Spain, 2014. ⟨http://sede.asturias.es/bopa/2014/04/21/2014–06617.pdf⟩ (accessed Nov 2023).

Bro, R., Smilde, A.K., 2014. Principal component analysis. Anal. Methods 6 (9), 2812–2831.

Camm, G.S., Glass, H.J., Bryce, D.W., Butcher, A.R., 2004. Characterisation of a mining-related arsenic-contaminated site, Cornwall, UK. J. Geochem. Explor. 82 (1-3), 1–15.

Cardinale, M., Brusetti, L., Quatrini, P., Borin, S., Puglia, A.M., Rizzi, A., Zanardini, E., Sorlini, C., Corselli, C., Daffonchio, D., 2004. Comparison of different primer sets for use in automated ribosomal intergenic spacer analysis of complex bacterial communities. Appl. Environ. Microbiol. 70 (10), 6.

Castaño, A., Prosenkov, A., Baragaño, D., Otaegui, N., Sastre, H., Rodríguez-Valdés, E., Gallego, J.L., Peláez, A.I., 2021. Effects of in situ remediation with nanoscale zero valence iron on the physicochemical conditions and bacterial communities of groundwater contaminated with arsenic. Front. Microbiol. 12, 580.

Chang, Y.T., Hseu, Z.Y., Zehetner, F., 2014. Evaluation of phytoavailability of heavy metals to Chinese cabbage (*Brassica chinensis L.*) in rural soils. Sci. World J. 2014, 309396.

Chung, H., Kim, M.J., Ko, K., Kim, J.H., Kwon, H.A., Hong, I., Kim, W., 2015. Effects of graphene oxides on soil enzyme activity and microbial biomass. Sci. Total Environ. 514, 307–313.

Clarke, K.R., Ainsworth, M., 1993. A method of linking multivariate community structure to environmental variables. Mar. Ecol. -Prog. Ser. 92, 205-205.

Corsi, I., Winther-Nielsen, M., Sethi, R., Punta, C., Della Torre, C., Libralato, G., Buttino, I., 2018. Ecofriendly nanotechnologies and nanomaterials for environmental applications: key issue and consensus recommendations for sustainable and ecosafe nanoremediation. Ecotoxicol. Environ. Saf. 154, 237–244.

De Cáceres, M., Legendre, P., Moretti, M., 2010. Improving indicator species analysis by combining groups of sites. Oikos 119 (10), 1674–1684.

Dermont, G., Bergeron, M., Mercier, G., Richer-Laflèche, M., 2008. Soil washing for metal removal: a review of physical/chemical technologies and field applications. J. Hazard. Mater. 152 (1), 1–31.

Dubey, R.K., Tripathi, V., Prabha, R., Chaurasia, R., Singh, D.P., Rao, C., Abhilash, P.C., 2020. Methods for exploring soil microbial diversity. In Unravelling the Soil Microbiome. Springer, Cham, pp. 23–32.

Dunnette, M.D., 1963. A modified model for test validation and selection research. J. Appl. Psychol. 47 (5), 317.

Efremova, L.V., Vasilchenko, A.S., Rakov, E.G., Deryabin, D.G., 2015. Toxicity of graphene shells, graphene oxide, and graphene oxide paper evaluated with Escherichia coli biotests. BioMed. Res. Int. 2015.

Fajardo, C., Costa, G., Nande, M., Martín, C., Martín, M., Sánchez-Fortún, S., 2019. Heavy metals immobilization capability of two iron-based nanoparticles (nZVI and Fe3O4): Soil and freshwater bioassays to assess ecotoxicological impact. Sci. Total Environ. 656, 421–432.

Fajardo, C., Sánchez-Fortún, S., Costa, G., Nande, M., Botías, P., García-Cantalejo, J., Martín, M., 2020. Evaluation of nanoremediation strategy in a Pb, Zn and Cd contaminated soil. Sci. Total Environ. 706, 136041.

Fang, J., Weng, Y., Li, B., Liu, H., Liu, L., Tian, Z., Du, S., 2022. Graphene oxide decreases the abundance of nitrogen cycling microbes and slows nitrogen transformation in soils. Chemosphere, 136642.

Fisher, M.M., Triplett, E.W., 1999. Automated approach for ribosomal intergenic spacer analysis of microbial diversity and its application to freshwater bacterial communities. Appl. Environ. Microbiol. 65 (10), 4630–4636.

Forstner, C., Orton, T.G., Skarshewski, A., Wang, P., Kopittke, P.M., Dennis, P.G., 2019. Effects of graphene oxide and graphite on soil bacterial and fungal diversity. Sci. Total Environ. 671, 140–148.

Frohne, T., Rinklebe, J., Diaz-Bone, R.A., Du Laing, G., 2011. Controlled variation of redox conditions in a floodplain soil: Impact on metal mobilization and biomethylation of arsenic and antimony. Geoderma 160 (3-4), 414–424.

Futalan, C.M., Phatai, P., Kim, J., Maulana, A.Y., Yee, J.J., 2019. Treatment of soil washing wastewater via adsorption of lead and zinc using graphene oxide. Environ. Sci. Pollut. Res. 26, 17292–17304.

Füzy, A., Kovács, R., Cseresnyés, I., Parádi, István, Szili-Kovács, T., Kelemen, B., Rajkai, K., Takács, T., 2019. Selection of plant physiological parameters to detect stress effects in pot experiments using principal component analysis. Acta Physiol. Plant 41, 56. https://doi.org/10.1007/s11738-019-2842-9aa.

Gallego, J.L.R., Verónica Peña-Álvarez, V., Lara, L.M., Baragaño, D., Forján, R., Colina, A., Prosenkov, A., Peláez, A.I., 2022. Effective bioremediation of soil from the Burgan oil field (Kuwait) using compost: A comprehensive hydrocarbon and DNA fingerprinting study. Ecotoxicol. Environ. Saf. 247, 114267.

Ganie, A.S., Bano, S., Khan, N., Sultana, S., Rehman, Z., Rahman, M.M., Khan, M.Z., 2021. Nanoremediation technologies for sustainable remediation of contaminated environments: Recent advances and challenges. Chemosphere 275, 130065.

Gong, Y., Chai, M., Ding, H., Shi, C., Wang, Y., Li, R., 2020. Bioaccumulation and human health risk of shellfish contamination to heavy metals and As in most rapid urbanized Shenzhen, China. Environ. Sci. Pollut. Res. 27 (2), 2096–2106.

Gower, J.C., 1975. Generalized procrustes analysis. Psychometrika 40 (1), 33–51.

Hazelton, P., Murphy, B., 2016. Interpreting soil test results: What do all the numbers mean. CSIRO publishing.

He, Y., Hu, R., Zhong, Y., Zhao, X., Chen, Q., Zhu, H., 2018. Graphene oxide as a water transporter promoting germination of plants in soil. Nano Res. 11 (4), 1928–1937.

Hill, M.O., 1973. Diversity and evenness: a unifying notation and its consequences. Ecology 54 (2), 427–432.

Houben, D., Evrard, L., Sonnet, P., 2013. Mobility, bioavailability and pH-dependent leaching of cadmium, zinc and lead in a contaminated soil amended with biochar. Chemosphere 92 (11), 1450–1457.

Hu, X., Kang, J., Lu, K., Zhou, R., Mu, L., Zhou, Q., 2014. Graphene oxide amplifies the phytotoxicity of arsenic in wheat. Sci. Rep. 4 (1), 1–10.

Janeiro-Tato, I., Antuña-Nieto, C., Lopez-Anton, M.A., Baragaño, D., Rodríguez, E., Peláez, A.I., Gallego, J.L.R., Martínez-Tarazona, M.R., 2021. Immobilization of mercury in contaminated soils through the use of new carbon foam amendments. Environ. Sci. Eur. 33, 127.

Kaiser, H.F., Rice, J., 1974. Little jiffy, mark IV. Educ. Psychol. Meas. 34 (1), 111–117.

Lê, S., Josse, J., Husson, F., 2008. FactoMineR: an R package for multivariate analysis. J. Stat. Softw. 25, 1–18.

Lei, Y., Chen, F., Luo, Y., Zhang, L., 2014. Synthesis of three-dimensional graphene oxide foam for the removal of heavy metal ions. Chem. Phys. Lett. 593, 122–127.

Lu, L., Wang, J., Chen, B., 2018. Adsorption and desorption of phthalic acid esters on graphene oxide and reduced graphene oxide as affected by humic acid. Environ. Pollut. 232, 505–513.

Mahamoud Ahmed, A., Lyautey, E., Bonnineau, C., Dabrin, A., Pesce, S., 2018. Environmental concentrations of copper, alone or in mixture with arsenic, can impact river sediment microbial community structure and functions. Front. Microbiol. 9, 1852.

Mantel, N., 1967. The detection of disease clustering and a generalized regression approach. Cancer Res. 27 (2 Part 1), 209–220.

Matos, M.P., Correia, A.A.S., Rasteiro, M.G., 2017. Application of carbon nanotubes to immobilize heavy metals in contaminated soils. J. Nanopart. Res. 19 (4), 1–11.

Mehlich, A., 1984. Mehlich 3 soil test extractant: a modification of mehlich 2 extractant. Commun. Soil Sci. Plant Anal. 15, 277–294.

Mench, M.J., Didier, V.L., Löffler, M., Gomez, A., Masson, P., 1994. A mimicked in-situ remediation study of metal-contaminated soils with emphasis on cadmium and lead. J. Environ. Qual. 23 (1), 58–63.

Ming, J., Sun, D., Wei, J., Chen, X., Zheng, N., 2019. Adhesion of bacteria to a graphene oxide film. ACS Appl. Bio Mater. 3 (1), 704–712.

Mishra, A.K., Ramaprabhu, S., 2011. Functionalized graphene sheets for arsenic removal and desalination of sea water. Desalination 282, 39–45.

Mohammadian, S., Krok, B., Fritzsche, A., Bianco, C., Tosco, T., Cagigal, E., Meckenstock, R.U., 2021. Field-scale demonstration of in situ immobilization of heavy metals by injecting iron oxide nanoparticle adsorption barriers in groundwater. J. Contam. Hydrol. 237, 103741.

Mondal, N.K., Chakraborty, S., 2020. Adsorption of Cr (VI) from aqueous solution on graphene oxide (GO) prepared from graphite: equilibrium, kinetic and thermodynamic studies. Appl. Water Sci. 10 (2), 1–10.

Motevalli, B., Parker, A.J., Sun, B., Barnard, A.S., 2019. The representative structure of graphene oxide nanoflakes from machine learning. Nano Futures 3 (4), 045001.

Naik, M.J.P., Debbarma, J., Saha, M., Bhargava, A., 2020. Graphene oxide nanoflakes from various agrowastes. Mater. Werkst. 51 (368), 2929.

Najafi, F., 2015. Removal of zinc (II) ion by graphene oxide (GO) and functionalized graphene oxide–glycine (GO–G) as adsorbents from aqueous solution: kinetics studies. Int. Nano Lett. 5 (3), 171–178.

Oksanen, J., 2012. Constrained Ordination: Tutorial with R and vegan. R. -Package Vegan 1–10.

Ramette, A., 2009. Quantitative community fingerprinting methods for estimating the abundance of operational taxonomic units in natural microbial communities. Appl. Environ. Microbiol. 75 (8), 2495–2505.

Ranjard, L., Echairi, A., Nowak, V., Lejon, D.P., Nouaïm, R., Chaussod, R., 2006. Field and microcosm experiments to evaluate the effects of agricultural Cu treatment on the density and genetic structure of microbial communities in two different soils. FEMS Microbiol. Ecol. 58 (2), 303–315.

RD 9/2005 (Royal Decree 9/2005), por el que se establece la relación de actividades potencialmente contaminantes del suelo y los criterios y estándares para la declaración de suelos contaminados, in English: ⟨https://www.miteco.gob.es/es/calidad-y-evaluacion-ambiental/temas/suelos-contaminados/09047122800b7aff_tcm30–194664.pdf⟩ (accessed Nov 2023).

Ren, W., Ren, G., Teng, Y., Li, Z., Li, L., 2015. Time-dependent effect of graphene on the structure, abundance, and function of the soil bacterial community. J. Hazard. Mater. 297, 286–294.

Revelle, M.W., 2015. Package 'psych'. Compr. R. Arch. Netw. 337, 338.

Roswell, M., Dushoff, J., Winfree, R., 2021. A conceptual guide to measuring species diversity. Oikos 130 (3), 321–338.

Shepard, R.N., 1962. The analysis of proximities: multidimensional scaling with an unknown distance function. I. Psychometrika 27 (2), 125–140.

Siddiqui, S.I., Chaudhry, S.A., 2018. A review on graphene oxide and its composites preparation and their use for the removal of As3+ and As5+ from water under the effect of various parameters: Application of isotherm, kinetic and thermodynamics. Process Saf. Environ. Prot. 119, 138–163.

Sitko, R., Turek, E., Zawisza, B., Malicka, E., Talik, E., Heimann, J., Wrzalik, R., 2013. Adsorption of divalent metal ions from aqueous solutions using graphene oxide. Dalton Trans. 42 (16), 5682–5689.

Song, B., Tang, J., Zhen, M., Liu, X., 2019b. Influence of graphene oxide and biochar on anaerobic degradation of petroleum hydrocarbons. J. Biosci. Bioeng. 128 (1), 72–79.

Song, Y., Kirkwood, N., Maksimović, Č., Zheng, X., O'Connor, D., Jin, Y., Hou, D., 2019a. Nature based solutions for contaminated land remediation and brownfield redevelopment in cities: A review. Sci. Total Environ. 663, 568–579.

Stankovich, S., Dikin, D.A., Dommett, G.H., Kohlhaas, K.M., Zimney, E.J., Stach, E.A., Ruoff, R.S., 2006. Graphene-based composite materials. Nature 442, 282–286.
Strawn, D.G., 2018. Review of interactions between phosphorus and arsenic in soils from four case studies. Geochem. Trans. 19 (1), 1–13.
Wang, H., Yuan, X., Wu, Y., Huang, H., Zeng, G., Liu, Y., Qi, Y., 2013. Adsorption characteristics and behaviors of graphene oxide for Zn (II) removal from aqueous solution. Appl. Surf. Sci. 279, 432–440.
Wang, J., Chen, B., 2015. Adsorption and coadsorption of organic pollutants and a heavy metal by graphene oxide and reduced graphene materials. Chem. Eng. J. 281, 379–388.
Williams, L.J., Abdi, H., 2010. Fisher's least significant difference (LSD) test. Encycl. Res. Des. 218, 840–853.
Wu, W., Yang, Y., Zhou, H., Ye, T., Huang, Z., Liu, R., Kuang, Y., 2013. Highly efficient removal of Cu (II) from aqueous solution by using graphene oxide. Water, Air, Soil Pollut. 224 (1), 1–8.
Xiong, T., Yuan, X., Wang, H., Leng, L., Li, H., Wu, Z., Zeng, G., 2018. Implication of graphene oxide in Cd-contaminated soil: a case study of bacterial communities. J. Environ. Manag. 205, 99–106.
Zhang, M., Gao, B., Chen, J., Li, Y., 2015. Effects of graphene on seed germination and seedling growth. J. Nanopart. Res. 17 (2), 1–8.
Zucconi, F., Pera, A., Forte, M., de Bertoldi, M.D., 1981. Evaluating toxicity of immature compost. BioCycle 22 (4), 54–57.
Zucconi, F., Monaco, A., Forte, M., de Bertoldi, M.D., 1985. Phytotoxins during the stabilization of organic matter. In: Gasser, J.K.R. (Ed.), Composting of Agricultural and other Wastes. Elsevier Applied Science Publication, New York, pp. 73–86.